Thermal conductivity and specific heat of glasses

Clare C. Yu
Los Alamos National Laboratory (T-11, Mail Stop B262), Los Alamos, New Mexico 87545
and Department of Physics, 1110 West Green Street, University of Illinois at Urbana-Champaign, Urbana, Illinois 61801

J. J. Freeman
Department of Physics, 1110 West Green Street, University of Illinois at Urbana-Champaign, Urbana, Illinois 61801
(Received 16 March 1987; revised manuscript received 16 July 1987)

We present a simple phenomenological model for glasses which fits both the thermal conductivity κ and the specific heat C up to roughly 100 K. This includes the plateau in κ as well as the maximum in C/T^3 which occur between 3–10 K. In addition to conventional tunneling systems and Rayleigh scattering, we introduce a sharp increase in the density of states due to local excitations. This feature is consistent with both Raman and neutron scattering. The absence of these states at low frequencies is due to interactions between the local modes and phonons.

Below 1K, a wide variety of amorphous materials exhibit[1] a specific heat C that varies linearly with temperature T and a thermal conductivity κ that increases as T^2. This behavior can be explained by assuming the existence of tunneling systems (TLS). At higher temperatures there is an anomalous specific heat, i.e., C/T^3 is about twice as large as one would predict for Debye phonons using the measured speed of sound. In fact, there is a bump in C/T^3 between 3 and 10 K. Glassy systems also have a plateau in their thermal conductivities which, for a given material, occurs at roughly the same temperature[2,3] as the maximum in C/T^3. At higher temperatures the thermal conductivity increases while C/T^3 decreases. Recent theoretical efforts to explain the thermal conductivity have included fractions[4] and phonon localization.[5–7] It is not obvious, however, in the first case how one can map a glass onto a self-similar percolating network, or in the second case how one can explain the rise in κ above the plateau.

In this paper we present a simply phenomenological model that fits both the specific heat and thermal conductivity data from low temperatures to about 100 K.[8] We start with the expression for the thermal conductivity

$$\kappa(T)=\tfrac{1}{3}\int_0^{\omega_D} C(T,\omega)vl(T,\omega)d\omega \ , \tag{1}$$

where $C(T,\omega)$ is the phonon specific heat, v is the velocity of sound, and $l(T,\omega)$ is the phonon mean free path. We are assuming that the heat is being carried by phonons. This has been experimentally verified[9] up to 10 K. One possible explanation for the plateau is to view it as a crossover from a low-frequency region ($\omega \lesssim 10^{11}$ Hz) with a long mean free path ($l \sim 150\lambda$) to a high-frequency region ($\omega \gtrsim 10^{12}$ Hz) with a short mean free path ($l \sim \lambda$) (Refs. 5, 6, and 10) as shown in Fig. 1. Here λ is the phonon wavelength. In the crossover region $l \propto \lambda^4$ as for Rayleigh scattering.[6,11]

To explain the decrease in mean free path at high frequencies, we make the ansatz, which we will justify later, that there is a sharp increase at energy E_0 in the density of states $n(E)$ of local excitations which scatter phonons. This enhancement accounts for both the rise in κ above the plateau and the anomalous specific heat. We will assume that these local modes can be described by Einstein oscillators[12] (EO) of energy E. For simplicity we take the density of states to be a unit step function

$$n(E)=n_0[1+S\Theta(E-E_0)] \ , \tag{2}$$

where S is te step height, n_0 is the constant TLS density of states which contribute to the specific heat, and $\Theta(E-E_0)$ is zero for $E<E_0$ and unity for $E>E_0$. The specific heat has contributions from conventional two-

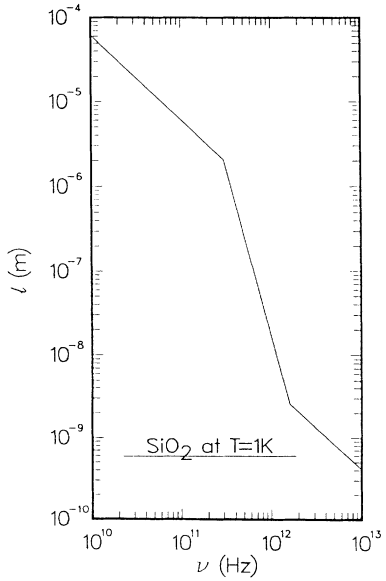

FIG. 1. Phonon mean free path as a function of frequency for vitreous SiO_2 at 1 K (Ref. 10).

level systems, local modes, and Debye phonons. Both the TLS and Einstein oscillators give rise to a specific heat that is linear in temperature but with different coefficients. Thus the maximum in C/T^3 may be viewed as a crossover from one to the other. Fits to the data are shown by the solid lines in Fig. 2 and the values of n_0 (calculated from fits to data below 1 K), E_0, and S_c are given in Table I. S_c is the step height associated with the specific heat. A better fit to the minima in C/T^3 could be obtained by noting that the low-temperature specific heat of insulating glasses is slightly superlinear, i.e., $C \sim T^{1+\epsilon}$ where $\epsilon > 0$.

We now consider the thermal conductivity. The total mean free path is given by the following expression:

$$l^{-1}(T,\omega) = \begin{cases} l^{-1}_{\text{res,TLS}}(T,\omega) + l^{-1}_{\text{rel,TLS}}(T,\omega) + l^{-1}_{\text{Rayleigh}}(T,\omega) & \text{for } \hbar\omega < E_0 \ , \\ l^{-1}_{\text{res,TLS}}(T,\omega) + l^{-1}_{\text{rel,TLS}}(T,\omega) + l^{-1}_{\text{res,EO}}(T,\omega) & \text{for } \hbar\omega > E_0 \ . \end{cases} \tag{3}$$

$l^{-1}_{\text{res,TLS}}(T,\omega)$ is due to resonant scattering of phonons from two-level systems,[20,21] and

$$l^{-1}_{\text{res,TLS}}(T,\omega) = \alpha\omega \tanh\left[\frac{\hbar\omega}{2k_B T}\right] , \tag{4}$$

where k_B is Boltzmann's constant and

$$\alpha = \frac{\pi \bar{P} \gamma^2}{\rho v^3} \ ,$$

$\bar{P}$ is the density of TLS states associated with thermal conductivity. In general $n_0/\bar{P} \sim 10$. The average coupling between TLS and the strain field is γ, and ρ is the mass density. $l^{-1}_{\text{rel,TLS}}(T,\omega)$ is due to TLS relaxation.[22] This arises because phonons perturb the energy-level separation and as a result the level population must readjust to a new equilibrium, and is given by

$$l^{-1}_{\text{rel,TLS}}(T,\omega) = \frac{\alpha}{\pi}\omega \int_0^\infty dx \frac{e^x}{(e^x+1)^2}\left[\frac{\pi}{2} - \tan^{-1}[\omega\tau_m(x)]\right] , \tag{5}$$

where $x = E/k_B T$,

$$\tau_m^{-1}(x) = \left[\frac{1}{v_l^5} + \frac{2}{v_t^5}\right]\frac{\gamma^2 k_B^3 T^3}{2\pi\rho\hbar^4} x^3 \coth\left[\frac{x}{2}\right] = A x^3 \coth\left[\frac{x}{2}\right]$$

is the maximum relaxation rate of a two-level system of energy E. For $\omega\tau_m \ll 1$,

$$l^{-1}_{\text{rel,TLS}} = \frac{\alpha}{4}\omega \ .$$

For $\omega\tau_m \gg 1$,

$$l^{-1}_{\text{rel,TLS}} = \frac{\pi^3}{16}\alpha A T^3 \ .$$

We have included Rayleigh scattering below the step in the form

$$l^{-1}_{\text{Rayleigh}}(T,\omega) = B\omega^4 \ , \tag{6}$$

where B is a constant. Although B may be given by several expressions[23,24] which involve, for example, fluctuations in the density or velocity, we will leave it as an adjustable parameter. Rayleigh scattering is only valid in the region $ka \lesssim 1$ where k is the phonon wave vector and a is the "size" of a scatterer. For convenience and to reduce the number of parameters in our model, we cut off the Rayleigh scattering at E_0. Table I shows that the value of $a = k^{-1} = \hbar v/E_0$ is consistently $\sim 25\%$ larger than the size[10] of a molecular unit δ. The fit would not change if we cut off the Rayleigh scattering at δ since it is insensitive to this parameter. Such a picture is consistent with neutron scattering experiment.[25] The strength of the Rayleigh scattering governs the low-temperature onset of the plateau. Without it E_0 could not have the same value for both the specific heat and thermal conductivity. For example, the plateau in amorphous SiO_2 would require a rise in $n(E)$ at 3 K whereas

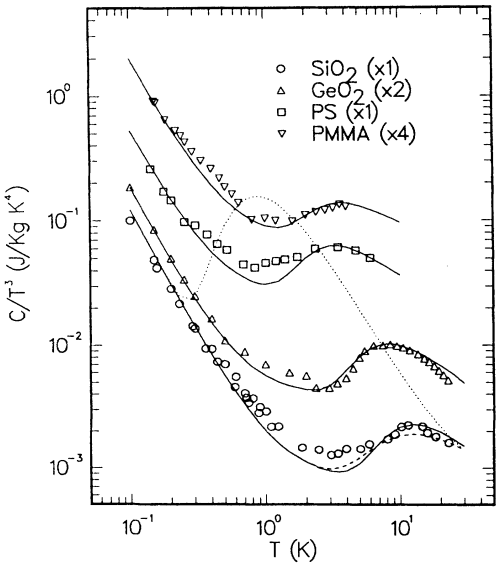

FIG. 2. Specific heat C divided by T^3. The solid lines are theoretical fits to the experimental data for SiO_2 (Refs. 13 and 14), GeO_2 (Refs. 14 and 15), polystyrene (PS) (Refs. 16 and 17), and polymethylmethacrylate (PMMA) (Refs. 16 and 17). The dashed line is derived using the density of states from neutron scattering (Ref. 18). The dotted line is calculated using the fit to the thermal conductivity of SiO_2 without Rayleigh scattering.

the maximum in C/T^3 demands an increase at 43 K. The effect of omitting Rayleigh scattering and moving the step to $E_0=3$ K is shown as the dotted lines in Figs. 2 and 3. If, however, Rayleigh scattering is not invoked, and $E_0=43$ K, the long-dash–short-dashed line in Fig. 3, results.

At frequencies above E_0 it is quite possible that the phonons probe the internal vibrational modes of the scatterers. We model these modes as Einstein oscillators. We take the Hamiltonian to be

$$H_{mn}=nE\delta_{mn}+\gamma_{mn}e(\delta_{m+1,n}+\delta_{m-1,n}) , \tag{7}$$

where e is the strain field, and n and m denote the energy levels of the oscillator. We assume for simplicity that the coupling $\gamma_{mn}=\gamma$, and that the coupling between phonons and Einstein oscillators is the same as that between phonons and TLS. We shall show later that this is physically reasonable. Phonons can cause resonant transitions between the oscillator levels. Resonant scattering from an infinite number of levels results in the temperature-independent expression

$$l^{-1}_{\text{res,EO}}(T,\omega)=\frac{2\alpha S_\kappa}{\pi}\omega . \tag{8}$$

We assume that to lowest order, phonons do not change the level separation. Thus we will neglect the relaxation contribution to l from the local modes. The resulting fits to the thermal conductivity data are shown in Fig. 3 and the parameters are listed in Table I. S_κ is the step height for the thermal conductivity. Since the fraction of SiO_2 units[1] involved in TLS is $\sim 10^{-4}$, the step heights cited in Table I imply that at most only a few percent of all the vibrational modes are involved in these local modes. In fitting C/T^3 and κ, we have used four adjustable parameters: E_0, S_κ, S_c, and B. Notice that the temperature and frequency dependence are not adjustable. S_κ, S_c, and B merely set the magnitude of their respective contributions and E_0 determines the frequency range in which the Rayleigh scattering and local modes contribute. The strength B of the Rayleigh scattering is that deduced from computer fits to the low-temperature data.[11] We have neglected structural relaxation which involves thermal activation of atoms over a potential barrier.[31] This mechanism involves frequencies which are orders of magnitude lower than those in which we are interested at a given temperature.

We will now justify the sharp rise in the density of states. This can be thought of as a hole at low frequencies, and is due to the interaction between the local modes and phonons. We now show that this interaction splits any degeneracy that might exist and we calculate the size of the resulting hole. Recall from degenerate perturbation theory that the energy shift E_{hole} is given by

$$\det|V_{nn'}-E_{\text{hole}}\delta_{nn'}|=0 , \tag{9}$$

where $V_{nn'}$ denote matrix elements of the perturbing interaction between the degenerate states n and n'. Setting $\gamma_{mn}=\gamma_{\text{hole}}$ in Eq. (7), we see that

$$V=\gamma_{\text{hole}}\hat{S}e , \tag{10}$$

TABLE I. Values of parameters used to fit the thermal conductivity and specific heat.

	E_0 (K)	S_κ	S_c	$B(10^{-45}$ s/cm)[c]	γ (eV)	γ_{hole} (eV)	$\bar{P}\gamma^2(10^8$ erg/cm^3)[c]	$n_0(10^{33}$/erg cm^3)[d]	$\frac{a}{\delta}$
SiO_2	43	235	460	16.5	0.3[a]	0.3	1.62	0.842	1.27
GeO_2	28	470	570	10.0	0.3[b]	0.2	0.86	1.03	1.21
polystyrene (PS)	11.2	220	195	603	0.09[a]	0.08	0.26	1.68	1.29
polymethylmethacrylate (PMMA)	12.5	360	110	368	0.09	0.09	0.16	1.83	1.31

[a]Reference 19.
[b]Reference 6.
[c]Consistent with Ref. 6.
[d]Reference 1.

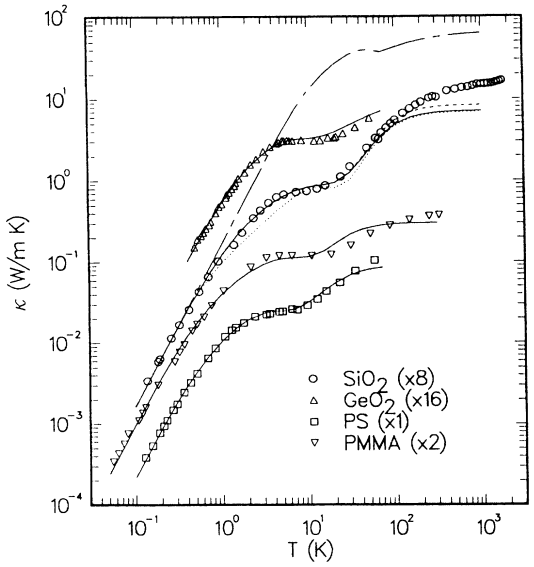

FIG. 3. Thermal conductivity κ of SiO_2 (Refs. 26 and 27), GeO_2 (Ref. 28), PS (Ref. 29), and PMMA (Ref. 30). The solid lines are calculated using infinite-level harmonic oscillators. The dashed line fitting the SiO_2 data is derived using the density of states from neutron scattering (Ref. 18). The dotted line is a fit to SiO_2 without Rayleigh scattering, and with $E_0=3$ K. (----) is for $E_0=43$ K, but again with the Rayleigh scattering term omitted.

where $\hat{S}$ is an operator acting on the local modes. For a two-mode system

$$\hat{S}=\hat{1}+\hat{\sigma}_x \ , \tag{11}$$

where $\hat{1}$ is the identity matrix and $\hat{\sigma}_x$ is one of the standard Pauli matrices. The strain field is given by

$$e=\nabla u(r)$$
$$=\frac{i}{\sqrt{\Omega}}\sum_k A\sqrt{k}\,(a_k e^{i\mathbf{k}\cdot\mathbf{r}}-a_k^\dagger e^{-i\mathbf{k}\cdot\mathbf{r}})\hat{\epsilon}_k \ , \tag{12}$$

where $\hat{\epsilon}_k$ is the polarization vector, Ω is the volume, $u(r)$ is the displacement, and

$$A=\left[\frac{\hbar}{2\rho v}\right]^{1/2} . \tag{13}$$

For simplicity set $\mathbf{r}=\mathbf{0}$. Then,

$$V=\frac{iA}{\sqrt{\Omega}}\gamma_{\text{hole}}(\hat{1}+\hat{\sigma}_x)\sum_k\sqrt{k}\,(a_k-a_k^\dagger)\hat{\epsilon}_k \ . \tag{14}$$

In Eq. (9), $|n\rangle$ and $|n'\rangle$ refer to degenerate states with the same number of phonons. Because V is linear in the strain field,

$$\langle n|V|n'\rangle=0 \ .$$

Thus $V_{nn'}$ should be replaced in Eq. (9) by second-order matrix elements, namely

$$V_{nn'}\rightarrow V_{nn'}^{(2)}=\sum_{m\neq(n,n')}\frac{V_{nm}V_{mn'}}{E_n^{(0)}-E_m^{(0)}} \ , \tag{15}$$

where m refers to states that are not degenerate with n and n'. They differ from n and n' in the number of phonons. Using Eq. (14) in Eq. (15), we find

$$V_{nn'}^{(2)}=\frac{2A^2\gamma_{\text{hole}}^2}{\Omega}\sum_k\frac{k}{-\hbar\omega_k}$$
$$=-\frac{\tilde{n}\gamma_{\text{hole}}^2}{\rho v^2} \ , \tag{16}$$

where $\tilde{n}=N/\Omega$. Since we are considering acoustic phonons which involve vibrations of the molecular units, N is the total number of molecular units. Thus $\tilde{n}=\delta^{-3}$. In Eq. (16) we have assumed that only one phonon polarization couples strongly to any particular set of local modes. Summing over all polarizations simply introduces a factor of 3. $V_{nn}^{(2)}$ is the same for $|n\rangle=|n'\rangle$ and $|n\rangle\neq|n'\rangle$. Substituting $V_{nn}^{(2)}$ for $V_{nn'}$ in Eq. (9), we find that the size of the hole in the density of states is given by

$$|E_{\text{hole}}|=\frac{2\gamma_{\text{hole}}^2}{\rho v^2\delta^3} \ . \tag{17}$$

Setting this equal to E_0, we obtain values of γ_{hole} which are in reasonable agreement with those deduced from thermal conductivity below 1 K. These are given in Table I. Notice that no such hole exists for conventional TLS since in that case phonons can either increase or decrease the level separation. For TLS the operator corresponding to $\hat{S}$ in Eq. (11) has $\hat{\sigma}_z$ in place of the identity matrix. Expressions similar to Eq. (17) can be found for multiple degenerate states. In general there will be different matrix elements connecting all the degenerate states. Again perturbation theory can be used to show that interactions with phonons splits this degeneracy and results in a hole in the density of states.

There is experimental evidence for the sharp increase in the density of states from both neutron[18] and Raman scattering.[32,33] Both indicate that the density of states has a dramatic rise at roughly the same frequency as we have deduced from the specific heat. Room-temperature Raman spectra, for example, exhibit a steep rise followed by a rounded peak and a more gradual fall off. This is the so-called boson peak which is characteristic of amorphous materials. The Raman intensity[34] is given by

$$\omega I(\omega)=\sum_i c_i(\omega)g_i(\omega)[n(\omega)+1] \ , \tag{18}$$

where the sum is over the different contributions to the intensity, $g_i(\omega)$ is the density of states of the ith excitation, $c_i(\omega)$ is the coupling of the phonons to the ith excitation, and $n(\omega)=[\exp(\hbar\omega/k_BT)-1]^{-1}$. Since there is no clear evidence for TLS from Raman scattering, we need only concern ourselves with phonons and our local modes. Since $c(\omega)$ depends on the strain-strain correlation function, we assume that it varies as ω^2. In order to explain the boson peak which has a room-temperature maximum around 52 cm^{-1} in amorphous SiO_2, Eq. (18) implies that the density of states must have more structure than a simple step function. If we use the density of states deduced from neutron scattering[18] in SiO_2, we can

obtain qualitative agreement with the measured Raman spectra. The resulting fits to the specific heat and thermal conductivity using the data of Ref. 18 are shown by the dashed lines in Figs. 2 and 3. Notice that the decreasing density of states reduces the thermal resistivity at high temperatures and improves the fit. We wish to emphasize that our use of the density of states from Ref. 18 does not imply our endorsement of the particular model of vibrational modes which was used to extract $g(\omega)$. We merely want to show that the experimental data from neutron scattering, Raman scattering, specific heat, and thermal conductivity are consistent with a sharp rise in the density of states of local excitations.

To our knowledge this is the first time that anyone has fit both the specific heat and thermal conductivity up to ~ 100 K with a single set of parameters. We have used conventional tunneling centers, a rather sudden onset of local modes modeled as Einstein oscillators, and Rayleigh scattering at frequencies below this onset. This does not solve the problem. Rather it helps to define it. The microscopic nature of these features is unknown. One can ask "At what length scale can one determine the difference between a glass and a crystal?" The existence of these modes implies that unlike the crystalline state, the amorphous state is characterized by well-defined excitations involving intermediate length scales which are larger than atomic dimensions but smaller than the size of the system. In other words, amorphous materials appear to have "clusters" of atoms. The operational definition of such a "cluster" is a group of atoms that can sustain local excitations with lifetimes much longer than their characteristic frequencies. Unlike other authors,[35] we define these energetically rather than structurally. If we were to excite a similar group of atoms in a crystal, the excitation would quickly decay into extended phonons and be very short lived. Clearly, any microscopic theory must include more than just phonons moving in a random static potential. It must also include the interactions between phonons and local dynamic structures.

We have enjoyed many illuminating discussions with A. C. Andersen. We thank Y. Fu for helpful suggestions and M. V. Klein for discussions on Raman scattering. This work was supported in part by National Science Foundation Grant No. DMR-83-16981 and by National Science Foundation (Low Temperature Physics Program) Grant No. DMR-86-13630.

[1]A general review may be found in *Amorphous Solids,* edited by W. A. Phillips (Springer, Berlin, 1981).

[2]D. P. Jones, J. Jackle, and W. A. Phillips, in *Phonon Scattering in Condensed Matter,* edited by H. J. Maris (Plenum, New York, 1980), p. 49, and references cited therein.

[3]D. A. Ackerman, D. Moy, R. C. Potter, A. C. Anderson, and W. N. Lawless, Phys. Rev. B **23**, 3886 (1981), and references cited therein.

[4]R. Orbach, J. Stat. Phys. **36**, 735 (1984).

[5]J. E. Graebner and B. Golding, Phys. Rev. B **34**, 5788 (1986).

[6]J. E. Graebner, B. Golding, and L. C. Allen, Phys. Rev. B **34**, 5696 (1986).

[7]E. Akkermans and R. Maynard, Phys. Rev. B **32**, 7850 (1985).

[8]Preliminary results have appeared in C. C. Yu and J. J. Freeman, in *Phonon Scattering in Condensed Matter V,* edited by A. C. Anderson and J. P. Wolfe (Springer, Berlin, 1986), p. 20.

[9]M. P. Zaitlin and A. C. Anderson, Phys. Rev. B **12**, 4475 (1975).

[10]J. J. Freeman and A. C. Anderson, Phys. Rev. B **34**, 5684 (1986).

[11]J. J. Freeman and A. C. Anderson, in *Phonon Scattering in Condensed Matter V,* edited by A. C. Anderson and J. P. Wolfe (Springer, Berlin, 1986), p. 32.

[12]Such a method has previously been applied to fit the maximum in C/T^3 only. See, for example, J. C. Lasjuanias and R. Maynard, J. Non-Cryst. Solids **6**, 101 (1971).

[13]J. C. Lasjaunias, A. Ravex, and M. Vandorpe, Solid State Commun. **17**, 1045 (1975).

[14]R. C. Zeller and R. O. Pohl, Phys. Rev. B **4**, (1971).

[15]A. A. Antoniou and J. A. Morrison, J. Appl. Phys. **36**, 1873 (1965).

[16]R. B. Stephens, Phys. Rev. B **8**, 2896 (1973).

[17]C. L. Choy, R. G. Hunt, and G. L. Salinger, J. Chem. Phys. **52**, 3629 (1970).

[18]U. Buchenau, N. Nücker, and A. J. Dianoux, Phys. Rev. Lett. **53**, 2316 (1984); **56**, 539(E) (1986); U. Buchenau, M. Pager, N. Nücker, A. J. Dianoux, N. Ahmad, and W. A. Phillips, Phys. Rev. B **34**, 5665 (1986).

[19]J.-Y. Duquesne and G. Bellessa, J. Phys. (Paris) Lett. **40**, L-193 (1979).

[20]P. W. Anderson, B. I. Halperin, and C. M. Varma, Philos. Mag. **25**, 1 (1972).

[21]W. A. Phillips, J. Low Temp. Phys. **7**, 351 (1972).

[22]J. Jackle, Z. Phys. **257**, 212 (1972).

[23]P. G. Klemens, Proc. Phys. Soc. London, Sect. A **68**, 73 (1955).

[24]C. L. Pekeris, Phys. Rev. **71**, 268 (1947).

[25]F. L. Galeenera and A. C. Wright, Solid State Commun. **57**, 677 (1986).

[26]T. L. Smith, Ph.D thesis, University of Illinois, 1975 (unpublished).

[27]Y. S. Touloukian, R. W. Powell, C. Y. Ho, and P. G. Klemens, *Thermophysical Properties of Matter* (Plenum, New York, 1970), Vol. 2, p. 193.

[28]K. Guckelsberger and J. C. Lasjaunias, Compt. Rend **270**, B1427 (1970).

[29]J. J. Freeman, Ph.D. thesis, University of Leeds, U.K., 1985 (unpublished).

[30]R. B. Stephens, G. S. Cieloszyk, and G. L. Salinger, Phys. Lett. **38A**, 215 (1972).

[31]S. Hunklinger and M. Von Schickfus, in *Amorphous Solids,* edited by W. A. Phillips (Springer, Berlin, 1981), p. 81.

[32]R. H. Stolen, Phys. Chem. Glasses **11**, 83 (1970).

[33]M. Hass, J. Phys. Chem. Solids **31**, 415 (1970).

[34]R. Shuker and R. W. Gamon, Phys. Rev. Lett. **25**, 222 (1970).

[35]J. C. Phillips, in *Solid State Physics,* edited by F. Seitz and D. Turnbull (Academic, New York, 1983), Vol. 37, p. 93.